



Low-amplitude, drifting sub-pulses hiding in background of noise-like pulse generated in fiber laser

JIACHEN WANG,^{1,2}  JUN HE,^{1,2,*}  CHANGRUI LIAO,^{1,2}  AND YIPING WANG^{1,2}

¹Key Laboratory of Optoelectronic Devices and Systems of Ministry of Education and Guangdong Province, College of Physics and Optoelectronic Engineering, Shenzhen University, Shenzhen 518060, China

²Guangdong and Hong Kong Joint Research Centre for Optical Fibre Sensors, Shenzhen University, Shenzhen 518060, China

*hejun07@szu.edu.cn

Abstract: We report a puzzling dynamic observed in a passively mode-locked fiber laser operating in the noise-like pulse regime, in which low-amplitude sub-structures emerge and drift away from the main waveform of the NLP pulse packet. The peak amplitudes of the drifting sub-pulses are orders of magnitude lower than the main packet when the NLP is monitored with a low-speed detecting system, a fact that makes the sub-pulses entirely hide in the background of the pulse train as the oscilloscope trace is displayed in a coarse amplitude resolution. Moreover, the presence of the low-amplitude sub-pulses cannot be detected in ordinary characteristics like optical spectrum, radio-frequency spectrum, and autocorrelation trace. We speculate that such a dynamic may extensively exist in fiber lasers operating in the noise-like pulse regime, and is just overlooked in the previous research efforts due to the difficulty to observe it. The discovery of this intriguing dynamic is informative for investigating the mechanisms of noise-like pulse.

© 2019 Optical Society of America under the terms of the [OSA Open Access Publishing Agreement](#)

1. Introduction

Passively mode-locked fiber lasers have been intensely studied over the past decades owing to their significances in a wide range of industrial and scientific applications [1]. A variety of operation regimes can be realized in mode-locked fiber lasers by governance of cavity dispersion, including conventional soliton, stretched pulse, dissipative soliton, similariton, etc [2]. In recent years, a peculiar mode-locking regime, noise-like pulse (NLP), has attracted great interest [3–12]. First demonstrated by Horowitz et al. at the close of the 1990's [3], NLP is not a single pulse but a pulse packet consisting of a bunch of ultra-short pulses with varying durations and peak intensities. The internal structure of the pulse packet is complex in which the ultra-short pulses are involved in chaotic motion, however as a whole the pulse packet conserves fairly stable global properties such as temporal envelope, average amplitude, energy, as well as the corresponding spectrum. On large time scale, the behavior of NLP is analogous to soliton, appearing as a steady train of pulse packets. The representative characteristic of NLP is its autocorrelation (AC) trace, which exhibits a double-scale structure with a narrow coherence peak riding on a broad pedestal. Another remarkable characteristic of NLP is its smooth and broad optical spectrum. NLP is a ubiquitous phenomenon that is observed in various dispersion regimes and laser architectures. Compared with solitary pulses, NLP features outstanding pulse energy (which can reach the level of μJ [13]), with a penalty of low coherence and longer duration. Such high energy, together with the broad spectrum, is attractive in certain application fields such as supercontinuum generation [14,15].

Hitherto the mechanisms behind the formation of NLP are still controversial. Due to the bandwidth limitation of the detecting system, the fine inner structure of NLP cannot be investigated

via experimental approaches. Although a number of theoretical modeling works are reported [16,17], a precise characterization of NLP remains challenging. In particular, the forms and dynamics of NLP are extremely rich, among which many cannot be well elucidated with the existing models. For example, it is found that NLP packet can exhibit a rectangular waveform that is almost identical with dissipative soliton resonance (DSR) pulse [18]. It is also found that a single NLP packet can split into multiple bunches, sometimes even generate harmonic mode-locking [11]. The origins of these phenomena are yet to be unveiled.

In 2015, Santiago-Hernandez et al. reported a particularly intriguing dynamic associated with NLP [19]. It is found that on unknown conditions, sub-structures are continually released from the main packet of NLP, and drift along the cavity. In many aspects, the dynamic is similar to soliton rain [20,21]. Although the dynamic is informative for understanding the nature of NLP, after the discovery of it very few following works are reported [13,22]. In [13], the authors observed the dynamic in a high-energy fiber laser, and gave no further attention to it since its effects on the global performance of the laser are negligible. On the other hand, the authors of [22] carried out a comprehensive investigation of the dynamic with statistical methods, and disclosed some important patterns regarding the evolution of the drifting sub-pulses. In [22], the authors challenged the widely accepted practice to label NLP as mode-locking, in view of that the NLP operation affected by such dynamic barely demonstrates any stationary characteristics.

At present, the dynamic introduced above is perceived as a rare phenomenon which occurs in unknown circumstances. In all reported cases the drifting sub-pulses are of peak amplitudes that are high enough to be observed easily. For example, in [19] the amplitudes of the sub-pulses are approximately half of the main packet as the oscilloscope trace is acquired with a detecting system (i.e., a photodetector and an oscilloscope) whose overall bandwidth is only 200 MHz. In this paper, we report a more interesting case in which the sub-pulses are of peak amplitudes that are much lower than the main packet of NLP. Owing to their low amplitudes, the sub-pulses are invisible as the oscilloscope trace is displayed in a large vertical scale (i.e., displayed in a coarse amplitude resolution); they entirely “hide” in the background of the pulse train. The phenomenon is particularly evident in the cases in which low-speed detecting systems are employed. When a detecting system of larger bandwidth is used, the measured amplitudes of the drifting sub-pulses increase, however they are still much lower than the main packet and are difficult to observe as the pulse train is displayed in a coarse amplitude resolution. Moreover, the existence of such low-amplitude sub-pulses cannot be detected in optical spectrum, radio-frequency (RF) spectrum, or AC trace. Besides the oscilloscope trace in a fine amplitude resolution, the NLP with the low-amplitude sub-pulses cannot be distinguished from the sub-pulse-free, “conventional” NLP in any characteristics. In the experimental works we found that the conventional NLP can be directly switched to the NLP with the low-amplitude sub-pulses by adjusting the polarization state. The discovery of the low-amplitude, drifting sub-pulses raises the issue that such dynamic may widely exist in NLP lasers, and is just overlooked previously due to the difficulty to detect it.

2. Experimental setup

The diagram of the experimental setup used in the present work is demonstrated in Fig. 1. The mode-locked fiber laser is established in an all-fiber architecture which employs nonlinear amplifying loop mirror (NALM) as the artificial saturable absorber. The NALM-based system adopts a figure-9 design [23] that is free of isolator, and therefore, permits the laser to operate under high power without exposing the components to the risk of optical damage. The gain medium of the laser is 1.5 m holmium (Ho) doped fiber, so the laser operates in the 2 μm wavelength region. The Ho-doped fiber is pumped with an in-house built thulium (Tm) doped fiber laser (TDFL) which delivers up to 3.69 W output at 1.95 μm . The pump radiation is injected into the amplifying loop of the NALM-based setup via a 1.95/2.1 μm wavelength-division multiplexer (WDM). The amplifying loop comprises the Ho-doped fiber and 30 m passive fiber.

The passive fiber is used to provide nonlinear phase shift for achieving mode-locking. A three paddle polarization controller (PC) is inserted between the passive fiber and the WDM for manipulating polarization. The amplifying loop is connected to two ports of a fiber coupler. To further enhance the nonlinear phase accumulation, the coupler is asymmetric (45/55). The other two ports of the coupler are used as the output port and the route to a 100% reflectivity fiber loop mirror, respectively. The 100% reflectivity fiber loop mirror is realized by splicing two ports of a 50/50 coupler. In view of that the 50/50 coupler cannot be perfectly symmetric, a light trap is connected to the idle port of the coupler for eliminating the transmitted radiation.

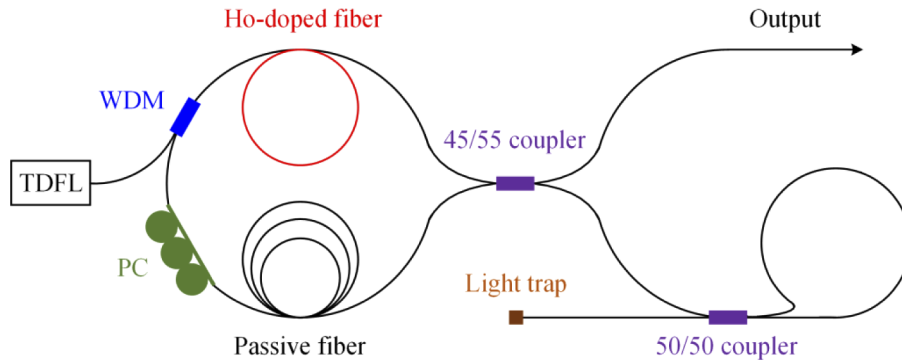


Fig. 1. Diagram of the figure-9 mode-locked Ho-doped fiber laser.

In the setup, all fibers are supplied by Nufern Inc (currently Coherent Inc). The models of the Ho-doped fiber and passive fiber are respectively SM-HDF-10/130 and SM-GDF-10/130-15M. Both fibers are of an anomalous dispersion of $-0.11 \text{ ps}^2/\text{m}$ at $2.1 \mu\text{m}$, which results in a net cavity dispersion of $\sim -6 \text{ ps}^2$ that is calculated from the total length of the cavity ($\sim 60 \text{ m}$). The model of the Tm-doped fiber used in the TDFL is SM-TDF-10P/130-HE. The TDFL is formed with the Tm-doped fiber and a pair of fiber Bragg gratings (FBG). The FBGs are inscribed on SM-GDF-10/130-15M fiber by O/E land Inc. The TDFL is pumped with a laser diode (maximum output power: 12 W) which is supplied by BWT Beijing Ltd. The WDM and couplers are fabricated with SM-GDF-10/130-15M fiber by AFR Ltd. The PC is supplied by KS photonics Inc, and is coiled with SM-GDF-10/130-15M fiber by us. The light trap is provided by Thorlabs Inc.

The output of the passively mode-locked Ho-doped fiber laser is characterized with the following equipments: optical spectrum analyzer (OSA, Yokogawa AQ6375B), oscilloscope (Tektronix MDO3054, bandwidth: 500 MHz; Teledyne LeCroy SDA 820Zi-B, bandwidth: 20 GHz), RF spectrum analyzer (Rohde & Schwarz FSV100), photodetectors (EOT ET-5000F, bandwidth: 12.5 GHz), and autocorrelator (Femtochrome FR-103XL).

3. Experimental results

Firstly we investigate the ordinary characteristics (optical spectrum, RF spectrum, AC trace, and pulse train) of the pulse generated by the figure-9 fiber laser to learn its general state. During the acquisitions of the characteristics, the output of the laser is divided by a 1/99 coupler. The 1% port of the coupler is connected to the oscilloscope whilst the 99% port is alternately connected to the OSA, RF spectrum analyzer, and autocorrelator. Hence, other characteristics are always simultaneously monitored with the oscilloscope trace.

Mode-locking is established by adjusting the paddles of the PC. Figure 2(a) demonstrates the optical spectrum of the mode-locking operation. The spectrum is broad and structureless, which is typical for NLP. The full width at half maxima (FWHM) of the spectrum is $\sim 18 \text{ nm}$. The

operation regime is identified based upon the AC trace presented in Fig. 2(b), which features a double scale structure with a narrow peak riding on a wide pedestal that extends beyond the maximum scan range of the autocorrelator (200 ps). Such an AC trace confirms that the generated pulse belongs to the family of NLP. The RF spectrum is shown in Fig. 2(c), which indicates that the fundamental repetition frequency of the laser is ~ 5.01 MHz. The relatively low signal-to-noise ratio (SNR) and the large sidelobes reflect the inherent timing jitter of NLP. The pulse train is illustrated in Fig. 2(d), which is registered using the 500-MHz oscilloscope (MDO3054) in a coarse amplitude resolution (200 mV/div). The NLP packets are equally spaced by ~ 199.5 ns, corresponding well to the 5.01 MHz repetition frequency.

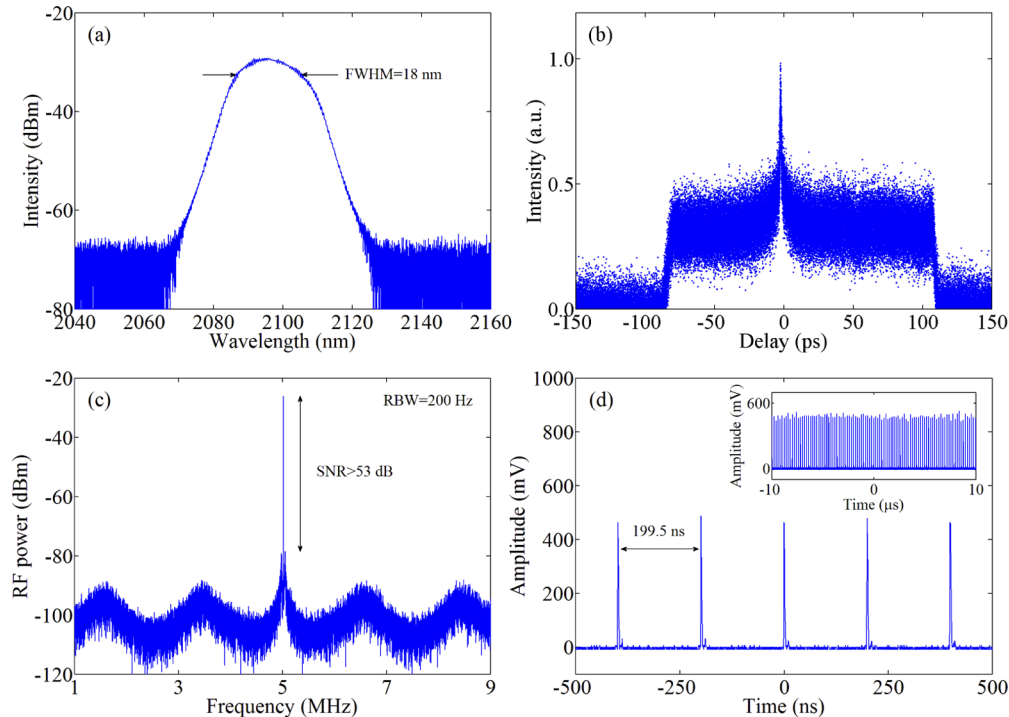


Fig. 2. Output characteristics of the mode-locked Ho-doped fiber laser: (a) optical spectrum, (b) AC trace, (c) RF spectrum, (d) pulse train recorded using the 500-MHz oscilloscope. Inset: pulse train in a 20 μ s span. All characteristics are measured under 3.69 W pump.

According to the characteristics presented in Fig. 2, the pulse generated by the figure-9 fiber laser appears to be a classic NLP. However, as the amplitude resolution of the oscilloscope is enhanced, sub-pulses in ceaseless motion are gradually observed (see [Visualization 1](#)). The details of the sub-pulses in a resolution of 5 mV/div are demonstrated in Fig. 3(a), which are extracted from the identical pulse train presented in Fig. 2(d). Such details cannot be reconstructed from the data registered in coarse amplitude resolutions. To store the information of the sub-pulses, the display of the oscilloscope trace must be zoomed in to scales in which the NLP packets cannot be entirely displayed, as shown in Fig. 3(b).

In the oscilloscope traces presented in Fig. 3, the tiny parasitic peaks adjacent to the main packets are induced by the imperfect impedance matching, and thus, are illusions which are irrelevant with the actual optical signal. During the acquisition of the traces, the main packet of NLP is set as trigger. The peak amplitudes of the sub-pulses detected by the 500-MHz oscilloscope are well below 10 mV [see Fig. 3(a)], whilst the peak amplitude of the main packet is almost 500 mV [see Fig. 2(d), which is registered from the identical pulse shown in Fig. 3(a)],

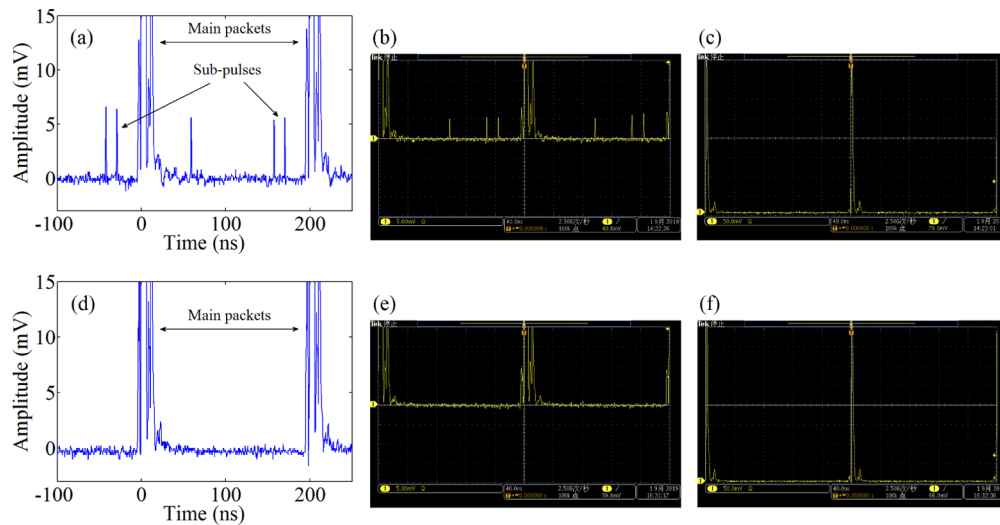


Fig. 3. Oscilloscope trace of the NLP with the drifting sub-pulses in various amplitude resolutions: (a), (b) 5 mV/div, (c) 50 mV/div. Oscilloscope trace of the conventional NLP in various amplitude resolutions: (d), (e) 5 mV/div, (f) 50 mV/div. See also [Visualization 1](#) and [Visualization 2](#). All traces (including the visualizations) are acquired using the 500-MHz oscilloscope.

that is two orders of magnitude higher than the sub-pulses. As a consequence, the drifting sub-pulses hide in the background of the pulse train as the oscilloscope trace is displayed in a coarse amplitude resolution (in other words, displayed in a large vertical scale). Figure 3(c) shows the pulse train of the NLP with the drifting sub-pulses in a resolution of 50 mV/div. In such a resolution, the main packets occupy (in practice, extend beyond) the whole displayer of the 500-MHz oscilloscope, whilst the sub-pulses are still invisible. Such a result is comprehensible given that the amplitudes of the sub-pulses are orders of magnitude lower than that of the main packets. To observe the low-amplitude sub-pulses, the display of the oscilloscope must be zoomed in. The advent of the sub-pulses through the adjustment of the display scale is demonstrated in [Visualization 1](#).

Via manipulating the polarization, a more stable NLP operation state which is free of the drifting sub-pulses is achieved using the figure-9 fiber laser. The manipulation can be realized by slightly changing the angle of any individual paddle of the PC. Figure 3(d) presents the details of this “conventional” NLP (recorded by the 500-MHz oscilloscope) in a resolution of 5 mV/div. Compared with Fig. 3(a), the sub-pulses are clearly absent in the conventional NLP operation state. [Visualization 2](#) demonstrates the oscilloscope trace of the sub-pulse-free NLP as the amplitude resolution is tuned from 50 mV/div [see Fig. 3(f)] to 5 mV/div [see Fig. 3(e)]. Throughout the tuning range of the display scale, no sub-pulses appear.

The presence of the conventional, sub-pulse-free NLP indicates that multiple NLP operation states can be established in the figure-9 setup, and these states are switchable by adjusting the intracavity polarization. As aforementioned, the optical spectrum, RF spectrum, and AC trace illustrated in Fig. 2 are acquired in the operation state bearing the drifting sub-pulses; this can be guaranteed by concurrently monitoring these characteristics with the oscilloscope trace in a fine amplitude resolution. It is desired to know whether these characteristics exhibit any features that can be used to distinguish their corresponding operation (i.e., the NLP with the low-amplitude, drifting sub-pulses) from the conventional NLP. Therefore, the characteristics acquired from the two states are compared.

The optical spectra of the NLP with the drifting sub-pulses and the conventional NLP are respectively presented in Figs. 4(a) and 4(c). The shapes of the two spectra are almost identical, with a tiny difference in the central wavelengths. The AC traces of the NLP with the drifting sub-pulses and the conventional NLP are respectively presented in Figs. 4(b) and 4(d). No significant difference between them is observed. Figure 5 demonstrates the RF spectra of the NLP with the drifting sub-pulses and the conventional NLP. There is no remarkable difference between the RF spectra, either in fundamental frequency or harmonics. In practice, the SNRs achieved in the two operation states are identical (~ 53 dB).

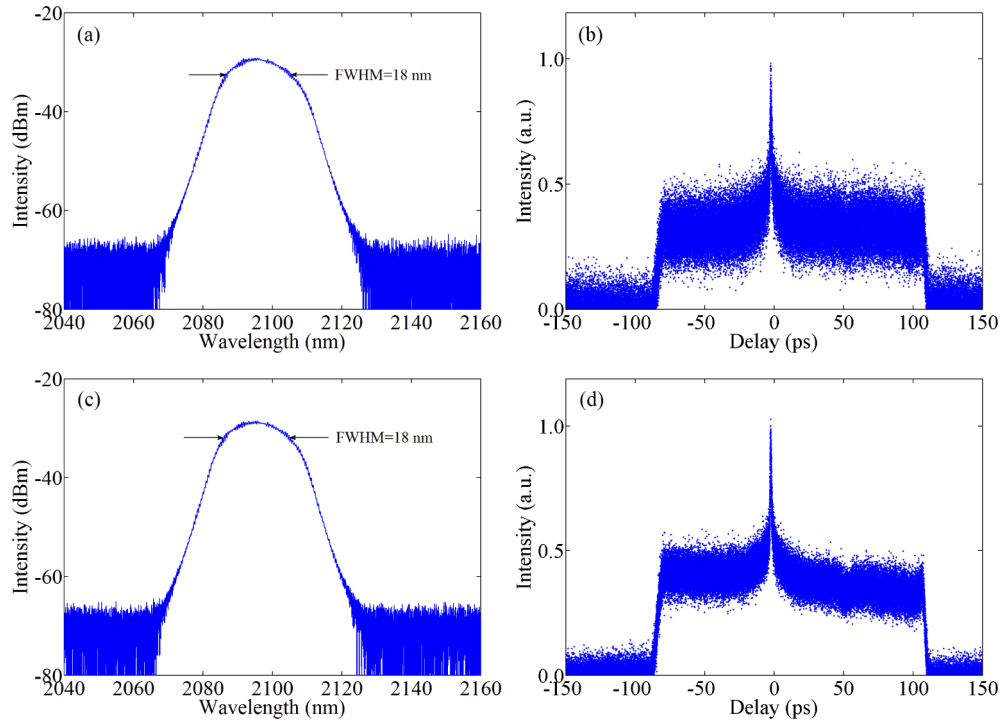


Fig. 4. Output characteristics of the NLP with the drifting sub-pulses: (a) optical spectrum, (b) AC trace. Output characteristics of the conventional NLP: (c) optical spectrum, (d) AC trace.

As presented above, the NLP with the low-amplitude, drifting sub-pulses cannot be distinguished from the conventional, sub-pulse-free NLP in ordinary characteristics like optical spectrum, RF spectrum, and AC trace. Such a result can be reasonably explained by the fact that the total energy of the sub-pulses is negligible compared with the energy of the main packet. In addition to their low peak amplitudes, the temporal widths of the sub-pulses are substantially narrower than the main packet. As a consequence, the energy possessed by the drifting sub-pulses is not sufficient to be detected in the ordinary characteristics. On the other hand, if the amplitudes of the sub-pulses are comparable to the main packet, like in the cases reported in [19] and [22], we speculate that the presence of the sub-pulses will have echo on the RF spectrum. Unfortunately, the RF spectrum is not provided in [19] and [22].

We notice that the durations of the drifting sub-pulses are beyond the detection ability of the 500-MHz oscilloscope in experimental works. The precise waveform of the sub-pulses cannot be reconstructed by the oscilloscope. Such a fact implies that the amplitudes of the sub-pulses are distorted as they are measured using the 500-MHz oscilloscope. In order to better understand the dynamic, a real-time oscilloscope with much larger bandwidth is employed to investigate

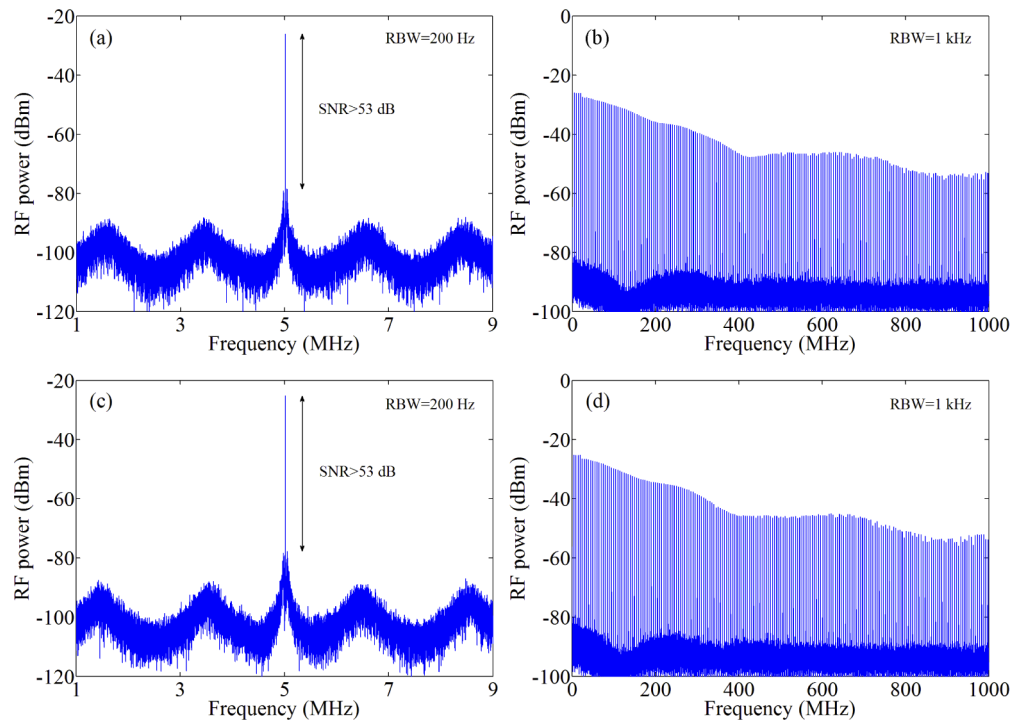


Fig. 5. RF spectrum of the NLP with the drifting sub-pulses: (a) around the fundamental frequency, (b) in a 1 GHz span. RF spectrum of the conventional NLP: (c) around the fundamental frequency, (d) in a 1 GHz span.

the drifting sub-pulses. The oscilloscope (SDA 820Zi-B) is capable of operating in multiple modes, of which the bandwidth is tunable from 20 MHz to 20 GHz. Firstly we set the mode to full bandwidth (i.e., 20 GHz). In such case, the detection ability is actually limited by the 12.5-GHz photodetector. The oscilloscope traces of the NLP with the drifting sub-pulses and the conventional NLP which are acquired using such a 12.5-GHz detecting system are presented in Fig. 6.

The amplitudes of the sub-pulses detected by the 12.5-GHz system are approximately 100 mV [see Fig. 6(a)], which is substantially higher than the value of 5 mV that is acquired with the 500-MHz system [see Fig. 3(a)]. Here the two values are obtained using different oscilloscopes (the 20-GHz SDA 820Zi-B and the 500-MHz MDO3054), however they can be reasonably compared given that the optical signal is received by the identical photodetector. The results indicate that there are considerable high-frequency components in the signal of the drifting sub-pulses which cannot be detected by low-speed detecting systems. Figure 6(b) shows the oscilloscope trace of the NLP with the drifting sub-pulses that is acquired using the 12.5-GHz system in an amplitude resolution of 200 mV/div. It is found that as the pulse is monitored in 12.5-GHz bandwidth, the sub-pulses are visible even in a coarse amplitude resolution; the sub-pulses cannot hide in the background of the main packet (see also Visualization 3). However, the difference between the amplitudes of the sub-pulses and the main packet is still huge. The oscilloscope traces of the conventional NLP acquired using the 12.5-GHz detecting system in fine and coarse resolutions are respectively presented in Figs. 6(c) and 6(d).

As demonstrated in Fig. 6, the visibility of the low-amplitude, drifting sub-pulses in coarse amplitude resolutions is strongly dependent on the performance of detecting systems. To further evaluate the influence of detecting systems, we compare the oscilloscope traces of the NLP with

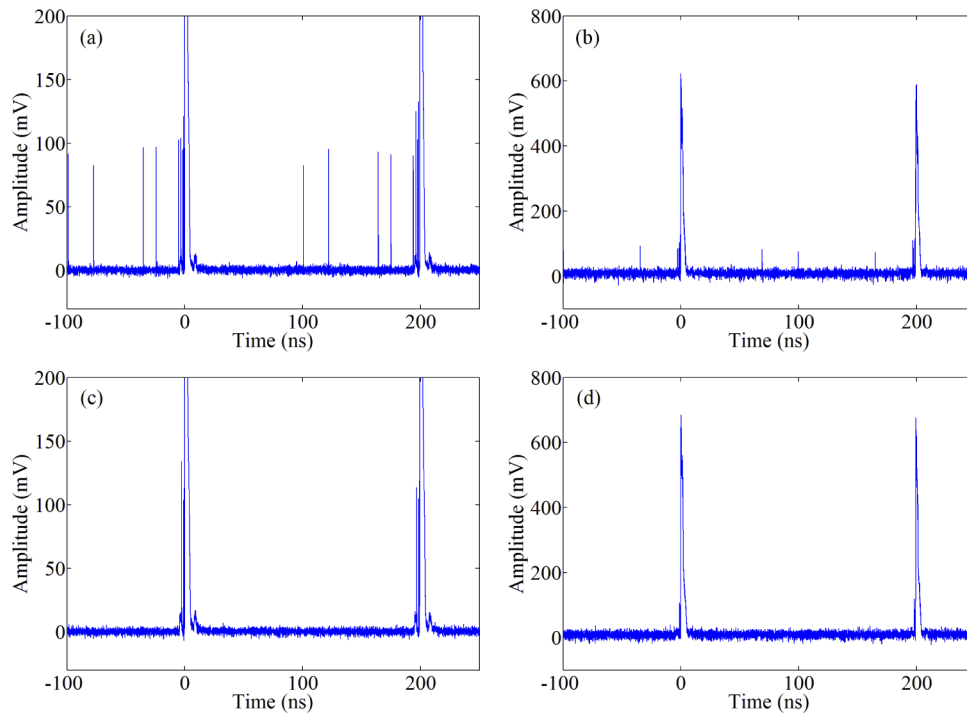


Fig. 6. Oscilloscope trace of the NLP with the drifting sub-pulses in various amplitude resolutions: (a) 50 mV/div, (b) 200 mV/div. See also [Visualization 3](#). Oscilloscope trace of the conventional NLP in various amplitude resolutions: (c) 50 mV/div, (d) 200 mV/div. All traces (including the visualization) are acquired using a 12.5-GHz detecting system.

the drifting sub-pulses acquired in different bandwidths (the bandwidth can be adjusted by setting the operation mode of the SDA 820Zi-B oscilloscope). The results are presented in Fig. 7. It is found that the detected amplitudes (and thus, the visibility) of the sub-pulses grow through the rising bandwidth. In an amplitude resolution of 200 mV/div, the sub-pulses become visible only after the bandwidth of the oscilloscope is raised above 4 GHz. Note that without offset, the 200-mV/div resolution corresponds to the smallest vertical scale to demonstrate the full waveform of the main packet on the display of the oscilloscope (see [Visualization 3](#)). The amplitude of the main packet also increases with the rising bandwidth, indicating that there are high-frequency components in the signal of the main packet which cannot be detected by low-speed detecting systems. As the oscilloscope trace is registered in the maximum available bandwidth (12.5 GHz), the amplitudes of the sub-pulses are still remarkably lower than that of the main packet (the ratio between the amplitudes of the sub-pulses and the main packet is roughly 1/6). It should be noted that the drifting sub-pulses reported in [19] are discovered with an oscilloscope whose bandwidth is only 200 MHz; using such a low-speed detecting system, the detected amplitudes of the sub-pulses reported in [19] are still almost half of the main packet. Hence, the actual difference between the amplitudes of the sub-pulses and the main packet observed in the present work is substantially larger than that reported in [19]. Another notable fact is that the precise waveform of the low-amplitude sub-pulses investigated in this paper cannot be recorded by the oscilloscope even in a bandwidth of 12.5 GHz, implying that the temporal widths of the sub-pulses are beyond the maximum detection ability of the detecting system (~ 100 ps). Therefore, the amplitudes measured using the 12.5-GHz system may be still lower than the actual values. Unfortunately, equipments with larger bandwidths are not available for us. On the

other hand, the increase of the bandwidth of the detecting system will induce the growth of noise (see Fig. 7), which is detrimental for measuring amplitudes.

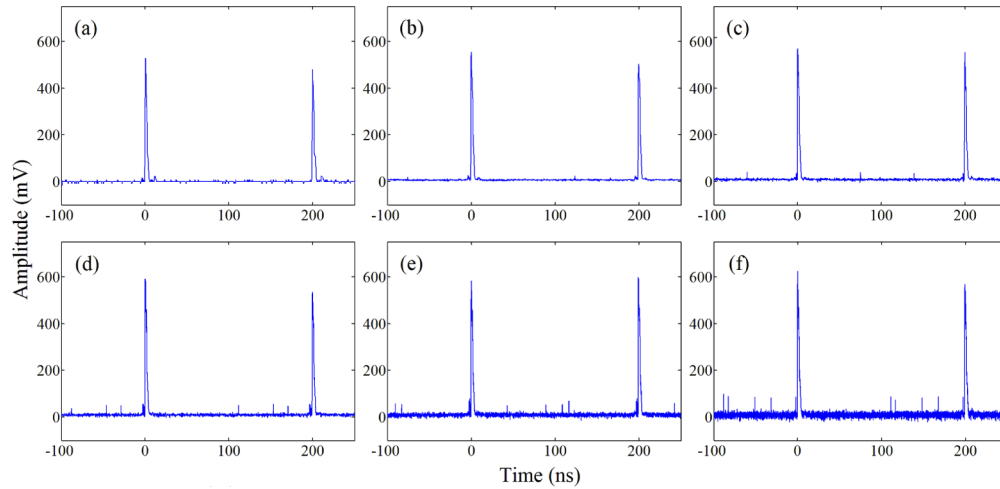


Fig. 7. Oscilloscope trace of the NLP with the drifting sub-pulses in an amplitude resolution of 200 mV/div which is acquired as the bandwidth of the oscilloscope is set to various modes: (a) 500 MHz, (b) 3 GHz, (c) 4 GHz, (d) 6 GHz, (e) 8 GHz, (f) 12.5 GHz.

In the experimental demonstrations, it is found that the trajectories of the drifting sub-pulses can be divided into two categories. In one category, the sub-pulses are released from the main packet and expelled away for a finite distance, and then abruptly vanish. In the other category the sub-pulses travel throughout the cavity. Such behaviors agree well with the phenomena reported in [19] and [22]. In [22], the amplitudes of the drifting sub-pulses are found to be distributed in a set of discrete, nearly equidistant values. The low-amplitude sub-pulses observed in our works also follow this pattern. By adjusting the PC, we can obtain operation modes in which the sub-pulses are of amplitudes distributed in a series of discrete values, as shown in Fig. 8. In particular, we observe a group of ultra-weak sub-pulses [see Figs. 8(a) and 8(b)]. The peak amplitudes of the ultra-weak sub-pulses (acquired with the 500-MHz oscilloscope) are below 3 mV (for comparison, the amplitudes of the common sub-pulses are ~ 6 mV), and they are involved in a puzzling periodical evolution. The ultra-weak sub-pulses undergo a step-like change to become the common sub-pulses in their next round trip, vice versa [see the inset of Fig. 8(a)]. Note that the period of one round trip is only ~ 199.5 ns, so the evolution is surprisingly fast. The mechanism behind this fast, periodical evolution is yet to be determined. We also investigate the ultra-weak sub-pulses using the 12.5-GHz detecting system [see Fig. 8(b)]. The mysterious periodical evolution is still observed. It is found that the difference between the amplitudes of the ultra-weak sub-pulses and the common sub-pulses become smaller as the data is acquired in 12.5-GHz bandwidth. Figures 8(c) and 8(d) show the oscilloscope traces of the NLP with prominent sub-pulses whose amplitudes are roughly twice of the common sub-pulses, in a bandwidth of 500 MHz and 12.5 GHz, respectively. Similarly, it is found that the difference between the amplitudes of the prominent sub-pulses and the common sub-pulses narrows as the data is acquired in larger bandwidth. The fact is further attested by recording the oscilloscope trace in various bandwidths. In [22], the authors report that the amplitudes of the drifting sub-pulses are distributed in a series of almost equidistant values. Our experimental results imply that the phenomenon is more complex.

In our works, the most frequently observed distribution pattern for the peak amplitudes of the sub-pulses is the one in which all sub-pulses share roughly equal amplitudes, as shown in

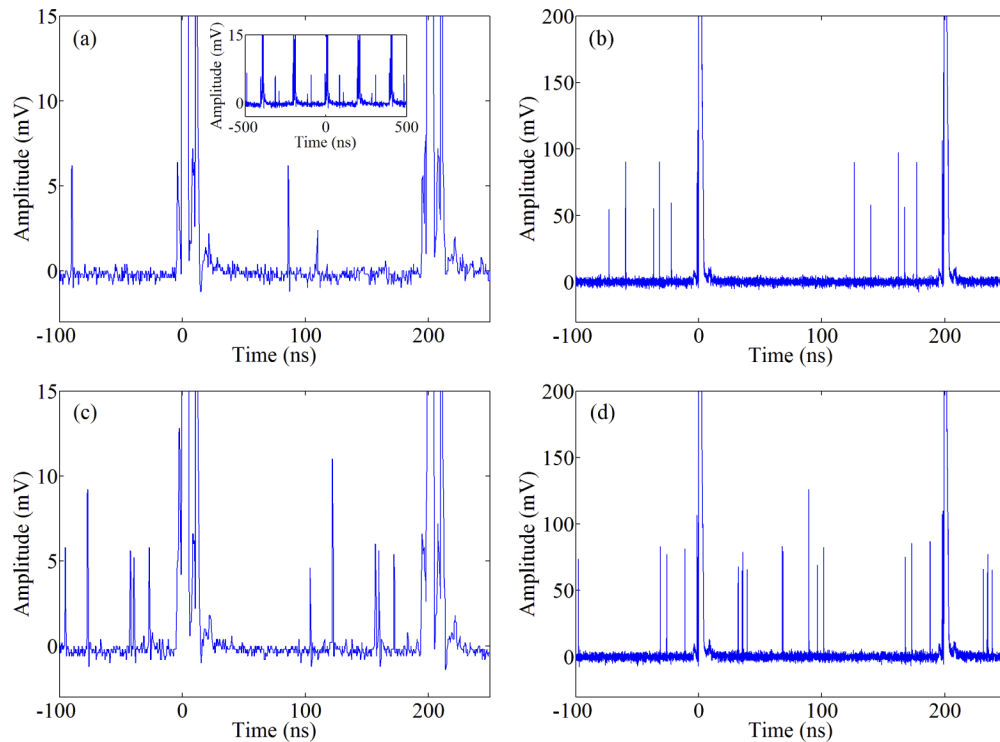


Fig. 8. (a) Oscilloscope trace of the NLP with the ultra-weak sub-pulses acquired using the 500-MHz detecting system. Inset: oscilloscope trace in a 1000 ns span. (b) Oscilloscope trace of the NLP with the ultra-weak sub-pulses acquired using the 12.5-GHz detecting system. (c) Oscilloscope trace of the NLP with the sub-pulses possessing amplitudes that are roughly twice of the common sub-pulses acquired using the 500-MHz detecting system. (d) Oscilloscope trace of the NLP with the sub-pulses possessing amplitudes that are roughly twice of the common sub-pulses acquired using the 12.5-GHz detecting system.

Visualization 1. Such a pattern is very stable, and can be maintained for hours without the occurrence of too high (or too low) amplitudes. The evolution of the sub-pulses following this pattern is presented in Fig. 9, which is registered using the 500-MHz oscilloscope by a single-shot capture of 4 ms, corresponding to ~ 20050 consecutive round trips. Figure 9(a) indicates that the peak amplitudes of the sub-pulses evolve in a limited range surrounding a central value which locates at ~ 6 mV. Restricted by the memory of the oscilloscope, the distribution of the amplitudes cannot be recorded for longer time by a single-shot capture. We instead made 10 captures with separation of 5 minutes. The result confirms the fact that the dominant peak amplitude of the sub-pulses is ~ 6 mV. Figure 9(b) depicts the trajectory of the sub-pulses which possess roughly equal amplitudes. The sub-pulses are released from the leading edge of the main packet, and propagate along the cavity until they are merged by the main packet again. It should be noted that the sub-pulses are released from the main packet in disorder. No regular pattern governing the interval between two sub-pulses is observed.

Finally, we investigate the stability of the two operation states (i.e., the NLP with the low-amplitude sub-pulses and the conventional NLP). Both states are found to be reproducible, as long as the paddles of the PC are fixed in the appropriate positions. Moreover, the two operation states can be maintained almost indefinitely. The oscilloscope trace of the NLP with the low-amplitude, drifting sub-pulses is monitored for hours. Throughout the monitoring, no degradation of the

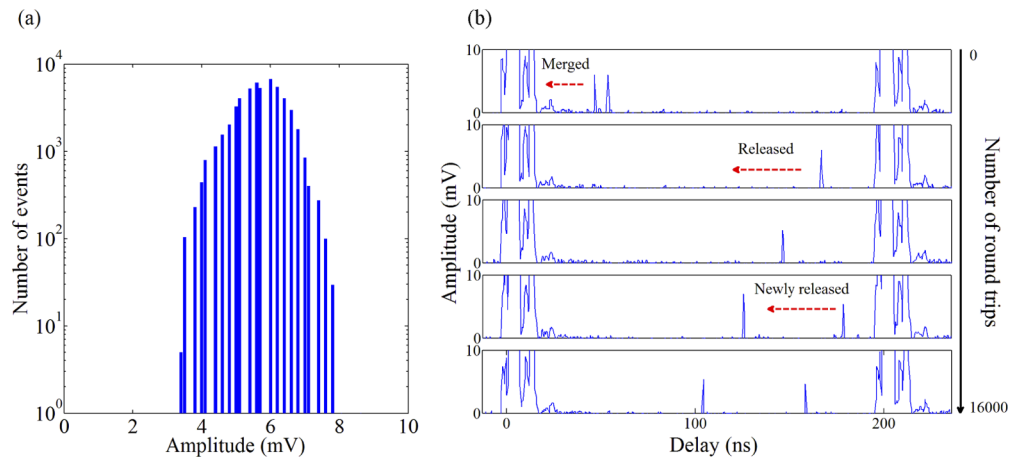


Fig. 9. (a) Histogram on a log-scale showing the distribution of the peak amplitudes of the drifting sub-pulses. (b) Trajectory of the drifting sub-pulses. Red arrow indicates the direction of motion. All data are acquired using the 500-MHz oscilloscope.

sub-pulses is observed. The long-term monitoring of the conventional NLP shows a similar steadiness, during which no onset of the sub-pulses is observed. Such facts indicate that without an adjustment of intracavity polarization, the two operation states cannot convert into each other spontaneously.

4. Discussion

Thus far, the mechanisms behind the formation of NLP are still under debate. Unlike conventional ultra-short pulses (soliton, similariton, etc) that are unitary, NLP bears complex, chaotic internal structure which results in extremely rich forms and dynamics. In particular, in a puzzling dynamic first reported by Santiago-Hernandez et al. in 2015, NLP is found to be capable of coexisting with ceaselessly drifting sub-pulses, a phenomenon that is analogous to soliton rain in many dimensions [19]. The discovery of this dynamic strongly challenges the common view that NLP is a steady operation state on large time scale [22].

The drifting sub-pulses reported in [19] and [22] are of amplitudes high enough to be detected easily using a very-low-speed oscilloscope whose bandwidth is 200 MHz. Obviously, such a phenomenon is very rare; few similar cases are reported after the discovery of it. Hence, the dynamic is perceived as a singular event which only occurs in some unknown circumstances. In the present paper, we discover that the dynamic can behave in a more subtle way, in which the drifting sub-pulses are of amplitudes that are significantly lower than the NLP packet. In such a case, the sub-pulses cannot be detected via common approaches. The optical spectrum, AC trace, and RF spectrum of the NLP with the low-amplitude sub-pulses cannot be distinguished from the conventional NLP which is free of the sub-pulses. Indeed, the low-amplitude drifting sub-pulses can be only observed in oscilloscope traces. Moreover, if the overall bandwidth of the detecting system (the oscilloscope and the photodetector) is not large enough, the sub-pulses are difficult to detect. When a low-speed detecting system is used, the sub-pulses will “hide” in the background of the pulse train as they are displayed in a large vertical scale that can accommodate the entire waveform of NLP packet.

The presence of the low-amplitude, drifting sub-pulses leads to the speculation that such a dynamic may widely occur in the NLP regime, instead of a special case. Due to their weak visibility, the low-amplitude sub-pulses are probable to be overlooked in the study of NLP, in view of that the high-speed detecting systems are not available for all researchers. Moreover,

the experimental results presented in this paper indicate that the switch from a “conventional” NLP to the NLP with the low-amplitude sub-pulses can be triggered by a slight change in the polarization state, and it induces no significant effects on the output characteristics of the laser. Therefore, many reported fiber lasers operating in the NLP regime may be accompanied by such low-amplitude sub-pulses.

The discovery of the low-amplitude, drifting sub-pulses reveals that NLP is an operation regime which is far from being well understood. In recent years, a number of non-solitary, long-duration pulse types are observed in mode-locked fiber lasers, including NLP [3–12], DSR [18], and h-shaped pulse [24]. Although they are considered by most researchers as stationary, or at least partially stationary mode-locking operation due to their soliton-like behavior on large time scale, the experimental results demonstrated in this paper implies that these pulse types deserve to be addressed more carefully. An investigation on the background of the oscilloscope trace in a fine amplitude resolution for these pulse types (DSR, h-shaped pulse, etc) is strongly desired.

Hitherto the mechanism behind the formation of the drifting sub-pulses in NLP is still unknown. Several probable causes of the dynamic have been discussed in [22], however a conclusion is yet to be reached. The dilemma is, to a large extent, attributed to the limited ability of the detecting systems. The exact temporal widths of the sub-pulses cannot be accurately measured, and consequently, the nature of the sub-pulses cannot be determined. In this work, the detection ability is restricted by the 12.5-GHz photodetector (the maximum available bandwidth of the SDA 820Zi-B oscilloscope is 20 GHz), using which we can only confirm that the durations of the sub-pulses are smaller than 100 ps. The authors of [19] and [22] provide the same estimation for the temporal widths of the sub-pulses (i.e., smaller than 100 ps). Such a broad range is insufficient to determine the nature of the sub-pulses, given that it can be met by either a bunch of pulses or a single pulse. If the essence of the sub-pulses is a small bunch of solitary pulses with an overall envelope narrower than 100 ps, then the formation of the sub-pulses is probable to be associated with the splitting of the main packet of NLP. In such case, the dynamic is induced by the large-scale instability of NLP, although the origin of the instability is unknown. On the other hand, if the sub-pulses are solitary pulses, the mechanism of the dynamic will be more complex. In such case, the drifting sub-pulses (assumed to be solitons) can be irrelevant with NLP (that is, the drifting sub-pulses and the main pulse of NLP are two independent events). The coexistence of NLP and soliton in the identical operation mode has been reported previously [25]. In [25], the central wavelengths of the soliton and the NLP are far apart, and thus, their presence can be easily recognized in the optical spectrum. If the central wavelengths of the two pulses are closer, the spectrum of the soliton can be completely covered by the spectrum of the NLP, given that the latter is usually broader. In a case that multiple solitons whose spectra are entirely covered by the spectrum of NLP chaotically emerge, one may observe a phenomenon which exhibits similar behavior with the dynamic reported in [19], [22] and this paper. Unfortunately, to identify such solitary pulses one has to address events with ultra-short durations, which is far beyond the detection ability of our equipments.

5. Conclusion

An intriguing dynamic which allows low-amplitude sub-pulses to be continually released and drift away from the main pulse packet is discovered in a mode-locked fiber laser operating in the NLP regime. The amplitudes of the drifting sub-pulses are substantially lower than the NLP packet. When a low-speed detecting system is used, the low-amplitude sub-pulses can entirely hide in the background of the pulse train as the oscilloscope trace is displayed in a coarse amplitude resolution. The presence of such low-amplitude sub-pulses cannot be recognized in ordinary characteristics like optical spectrum, RF spectrum, and AC trace. We hold the view that such a dynamic may extensively exist in fiber lasers operating in the NLP regime, and is just overlooked in the previous research efforts due to the difficulty to detect it.

Funding

National Natural Science Foundation of China (61875128, 61635007); Science and Technology Innovation Commission of Shenzhen (JCYJ20180305125352956, JCYJ20180507182058432, JCYJ20160427104925452); Development and Reform Commission of Shenzhen Municipality Foundation.

Acknowledgments

The authors would like to acknowledge Prof. Peiguang Yan, and Dr. Jinzhang Wang, for their helpful comments.

Disclosures

The authors declare no conflicts of interest.

References

1. M. E. Fermann, A. Galvanauskas, G. Sucha, and D. Harter, "Fiber-lasers for ultrafast optics," *Appl. Phys. B: Lasers Opt.* **65**(2), 259–275 (1997).
2. R. I. Woodward, "Dispersion engineering of mode-locked fibre lasers," *J. Opt.* **20**(3), 033002 (2018).
3. M. Horowitz, Y. Barad, and Y. Silberberg, "Noiselike pulses with a broadband spectrum generated from an erbium-doped fiber laser," *Opt. Lett.* **22**(11), 799–801 (1997).
4. D. Tang, L. Zhao, and B. Zhao, "Soliton collapse and bunched noise-like pulse generation in a passively mode-locked fiber ring laser," *Opt. Express* **13**(7), 2289–2294 (2005).
5. L. M. Zhao and D. Y. Tang, "Generation of 15-nJ bunched noise-like pulses with 93-nm bandwidth in an erbium-doped fiber ring laser," *Appl. Phys. B: Lasers Opt.* **83**(4), 553–557 (2006).
6. L. M. Zhao, D. Y. Tang, J. Wu, X. Q. Fu, and S. C. Wen, "Noise-like pulse in a gain-guided soliton fiber laser," *Opt. Express* **15**(5), 2145–2150 (2007).
7. S. Kobtsev, S. Kukarin, S. Smirnov, S. Turitsyn, and A. Latkin, "Generation of double-scale femto/pico-second optical lumps in mode-locked fiber lasers," *Opt. Express* **17**(23), 20707–20713 (2009).
8. A. K. Zaytsev, C. H. Lin, Y. J. You, F. H. Tsai, C. L. Wang, and C. L. Pan, "A controllable noise-like operation regime in a Yb-doped dispersion-mapped fiber ring laser," *Laser Phys. Lett.* **10**(4), 045104 (2013).
9. X. He, A. Luo, Q. Yang, T. Yang, X. Yuan, S. Xu, Q. Qian, D. Chen, Z. Luo, W. Xu, and Z. Yang, "60 nm bandwidth, 17 nJ noiselike pulse generation from a thulium-doped fiber ring laser," *Appl. Phys. Express* **6**(11), 112702 (2013).
10. Y. Mshiko, E. Fujita, and M. Tokurakawa, "Tunable noise-like pulse generation in mode-locked Tm fiber laser with a SESAM," *Opt. Express* **24**(23), 26515–26520 (2016).
11. J. P. Lauterio-Cruz, J. C. Hernandez-Garcia, O. Pottiez, J. M. Estudillo-Ayala, E. A. Kuzin, R. Rojas-Laguna, H. Santiago-Hernandez, and D. Jauregui-Vazquez, "High energy noise-like pulsing in a double-clad Er/Yb figure-of-eight fiber laser," *Opt. Express* **24**(13), 13778–13787 (2016).
12. G. Liu, K. Yin, L. Yang, Z. Cai, B. Zhang, and J. Hou, "Noise-like pulse generation from a Ho-doped fiber laser based on nonlinear polarization rotation," *Proc. SPIE* **10619**, 1061908 (2018).
13. X. Zhou, Z. Cheng, Y. Shi, H. Guo, and P. Wang, "High-energy noiselike pulses in an all-PM double-clad Er/Yb-codoped fiber laser," *IEEE Photonics Technol. Lett.* **30**(11), 985–988 (2018).
14. J. C. Hernandez-Garcia, O. Pottiez, and J. M. Estudillo-Ayala, "Supercontinuum generation in a standard fiber pumped by noise-like pulses from a figure-eight fiber laser," *Laser Phys.* **22**(1), 221–226 (2012).
15. A. Zaytsev, C. H. Lin, Y. J. You, C. C. Chung, C. L. Wang, and C. L. Pan, "Supercontinuum generation by noise-like pulses transmitted through normally dispersive standard single-mode fibers," *Opt. Express* **21**(13), 16056–16062 (2013).
16. G. M. Donovan, "Dynamics and statistics of noise-like pulses in modelocked lasers," *Phys. D* **309**, 1–8 (2015).
17. S. Smirnov and S. Kobtsev, "Modelling of noise-like pulses generated in fibre lasers," *Proc. SPIE* **9732**, 97320S (2016).
18. Z. Deng, G. Zhao, J. Yuan, J. Lin, H. Chen, H. Liu, A. Luo, H. Cui, Z. Luo, and W. Xu, "Switchable generation of rectangular noise-like pulse and dissipative soliton resonance in a fiber laser," *Opt. Lett.* **42**(21), 4517–4520 (2017).
19. H. Santiago-Hernandez, O. Pottiez, M. Duran-Sanchez, R. I. Alvarez-Tamayo, J. P. Lauterio-Cruz, J. C. Hernandez-Garcia, B. Ibarra-Escamilla, and E. A. Kuzin, "Dynamics of noise-like pulsing at sub-ns scale in a passively mode-locked fiber laser," *Opt. Express* **23**(15), 18840–18849 (2015).
20. S. Chouli and P. Grelu, "Rains of solitons in a fiber laser," *Opt. Express* **17**(14), 11776–11781 (2009).
21. S. Chouli and P. Grelu, "Soliton rains in a fiber laser: an experimental study," *Phys. Rev. A* **81**(6), 063829 (2010).
22. E. Garcia-Sanchez, O. Pottiez, Y. Bracamontes-Rodriguez, J. P. Lauterio-Cruz, H. E. Ibarra-Villalon, J. C. Hernandez-Garcia, M. Bello-Jimenez, and E. A. Kuzin, "Complex dynamics of a fiber laser in non-stationary pulsed operation," *Opt. Express* **24**(17), 18917–18930 (2016).

23. K. Krzempek, J. Sotor, and K. Abramski, "Compact all-fiber figure-9 dissipative soliton resonance mode-locked double-clad Er:Yb laser," *Opt. Lett.* **41**(21), 4995–4998 (2016).
24. J. Zhao, L. Li, L. Zhao, D. Tang, and D. Shen, "Cavity-birefringence-dependent h-shaped pulse generation in a thulium-holmium-doped fiber laser," *Opt. Lett.* **43**(2), 247–250 (2018).
25. O. Pottiez, H. E. Ibarra-Villalon, Y. Bracamontes-Rodriguez, J. A. Minguela-Gallardo, E. Garcia-Sanchez, J. P. Lauterio-Cruz, J. C. Hernandez-Garcia, M. Bello-Jimenez, and E. A. Kuzin, "Soliton formation from a noise-like pulse during extreme events in a fibre ring laser," *Laser Phys. Lett.* **14**(10), 105101 (2017).